Surface-Grafted Polysarcosine as a Peptoid Antifouling Polymer Brush

ARTICLE *in* LANGMUIR · OCTOBER 2012

Impact Factor: 4.46 · DOI: 10.1021/la302131n · Source: PubMed

Langmuir

Article

pubs.acs.org/Langmuir

Surface-Grafted Polysarcosine as a Peptoid Antifouling Polymer Brush

King Hang Aaron Lau,[†,‡] Chunlai Ren,[○] Tadas S. Sileika,[†,‡] Sung Hyun Park,[†,‡] Igal Szleifer,*[,†,‡,§,∥,⊥] and Phillip B. Messersmith*[,†,‡,∥,⊥,#,▽]

[†]Department of Biomedical Engineering, [‡]Chemistry of Life Processes Institute, [§]Department of Chemistry, [∥]Department of Chemical and Biological Engineering, [⊥]Robert H. Lurie Comprehensive Cancer Center, [#]Institute for Bionanotechnology in Medicine, and [▽]Department of Materials Science and Engineering, Northwestern University, Evanston, Illinois 60208, United States

[○]National Laboratory of Solid State Microstructures, Nanjing University, Nanjing 210093, China

Supporting Information

ABSTRACT: Poly(*N*-substituted glycine) "peptoids" are a class of peptidomimetic molecules receiving significant interest as engineered biomolecules. Sarcosine (i.e., poly(*N*-methyl glycine)) has the simplest side chain chemical structure of this family. In this Article, we demonstrate that surface-grafted polysarcosine (PSAR) brushes exhibit excellent resistance to nonspecific protein adsorption and cell attachment. Polysarcosine was coupled to a mussel adhesive protein-inspired DOPA-Lys pentapeptide, which enabled solution grafting and control of the surface chain density of the PSAR brushes. Protein adsorption was found to decrease monotonically with increasing grafted chain densities, and protein adsorption could be completely inhibited above certain critical chain densities specific to different polysarcosine chain lengths. The dependence of protein adsorption on chain length and density was also investigated by a molecular theory. PSAR brushes at high chain length and density were shown to resist fibroblast cell attachment over a 7 week period, as well as resist the attachment of some clinically relevant bacterial strains. The excellent antifouling performance of PSAR may be related to the highly hydrophilic character of polysarcosine, which was evident from high-pressure liquid chromatography measurements of polysarcosine and water contact angle measurements of the PSAR brushes. Peptoids have been shown to resist proteolytic degradation, and polysarcosine could be produced in large quantities by *N*-carboxy anhydride polymerization. In summary, surface-grafted polysarcosine peptoid brushes hold great promise for antifouling applications.

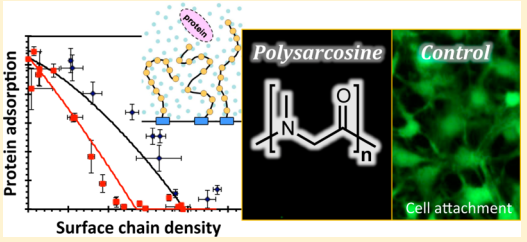

1. INTRODUCTION

Protein adsorption and subsequent cell−surface interactions constitute the acute biological response to biomedical materials. It is therefore hypothesized that an antifouling surface design that can prevent nonspecific protein adsorption and cell attachment may be able to improve the performance of a range of biomedical devices.[1−6] For example, surface-induced thrombosis initiated by plasma protein adsorption, and the activation of the coagulation system, are major complications in blood-contacting devices (e.g., small-diameter, synthetic vascular grafts and cardiac valve prosthetics).[7−9] The nonspecific adsorption of plasma proteins also recruits various cells involved in immunological cascades that lead to chronic inflammation and fibrous encapsulation of orthopedic and other biomedical devices.[10,11] Medical device-related infection caused by bacterial adhesion and biofilm formation affects a significant number of patients.[12−14] Nanoparticle theragnostics, biosensors, and tissue engineering constructs that deploy biorecognition elements also require an "inert" background surface free from nonspecific adsorption for optimal function.[15−17]

Peptide-based surfaces, such as oligopeptide self-assembled monolayers[18] and serum albumin blocking layers,[19,20] have been proposed for antifouling applications. However, such surfaces can be proteolytically degraded, and their long-term in vivo application is limited. Poly(*N*-substituted glycine) "peptoids" are a class of peptidomimetic molecules receiving significant interest as bioactive peptide mimics.[21−23] In contrast to peptides, peptoid side chains are attached to the backbone nitrogen to form tertiary amide bonds. This shift in the side chain position is believed to be responsible for the ability of peptoids to resist protease degradation,[21,24,25] and peptoids could therefore be advantageous for long-term biomedical applications such as antifouling material coatings.

Surface-grafted water-soluble polymer brushes are actively being investigated as antifouling surfaces. Such surface brushes present large energetic barriers, constituted by the balance between volume exclusion, conformational entropy, and segment interactions of the polymer brush, that must be overcome for protein adsorption to occur on the brush-functionalized surface.[26−28] A range of polymers have been demonstrated as antifouling surface brushes, including poly-

Received: May 24, 2012
Revised: September 30, 2012
Published: October 26, 2012

(ethylene glycol) (PEG),[29−31] zwitterionic designs,[32−35] and various surface-initiated polymerizable systems.[36−38] Peptoid systems have been relatively unexplored: a β-peptoid system has been investigated,[39] and our previous research demonstrated the antifouling performance of peptoid polymers with PEG-inspired methoxyethyl and hydroxypropyl side chains.[40−43]

Polysarcosine (i.e., poly(*N*-methyl glycine)), with only methyl groups as side chains, is the elementary peptoid in terms of the complexity in side chain chemical structure. It has been used as the hydrophilic block in amphiphilic peptoid block copolymers,[44,45] and model peptide studies have found that sarcosine substitutions in a peptide sequence are far more hydrophilic than alanine and even lysine residues.[46] Lacking chiral centers and intramolecular hydrogen bonds (no hydrogen-bond donors), polysarcosine has also long served as a model for studying peptide secondary structure formation,[47−49] and is found to possess relatively flexible backbone twist angles.[50] A lack of hydrogen-bond donors is also considered to be a beneficial characteristic in conferring resistance to protein adsorption,[2] and a tri(sarcosine)-terminated alkyl-thiol self-assembled monolayer has been found to exhibit remarkable antifouling properties.[51] We therefore hypothesize that the water-soluble polysarcosine, when surface-grafted as a polymer brush, would be an excellent peptidomimetic antifouling surface design.

In this Article, we present an evaluation of the antifouling performance of polysarcosine brushes in terms of the resistance against protein adsorption as well as in vitro cell attachment. Polysarcosine polymers were synthesized with a submonomer solid-phase synthesis protocol to precisely control the chain length, and to couple polysarcosine with a proven mussel adhesive protein-inspired DOPA-Lys surface anchor (DOPA = 3,4-dihydroxyphenylalanine; Lys = lysine) for convenient control of the grafting chain density.[43] The interaction of the polymer with water was characterized by reverse-phase high-pressure liquid chromatography (RP-HPLC), and surface wetting of the grafted polymer brush was characterized by dynamic water contact angle measurements. The DOPA-Lys surface anchor enabled the measurement of protein adsorption as a function of the grafted chain density and the identification of the critical density[43] for inhibiting protein adsorption. We also employed a molecular theory we previously introduced[26,42,43] to characterize the polymer−protein interaction. Finally, the long-term resistance of the polysarcosine brush surface against mammalian cell attachment over several weeks, and the resistance against attachment of three bacterial strains, were characterized. Our results show that polysarcosine is a promising antifouling polymer and suggest that this simplest of peptoids may confer outstanding antifouling properties.

2. EXPERIMENTAL SECTION

2.1. Materials. All chemical reagents and buffer salts were sourced from Aldrich (Milwaukee, WI) at ACS reagent grade or higher. High-purity solvents were purchased from VWR (Radnor, PA). Solid-phase peptide synthesis reagents (Rink amide-MBHA resin LL, HBTU, Fmoc-Lys(Boc)-OH, Fmoc-DOPA(acetonide)-OH, Fmoc-Ala-OH) were purchased from Novabiochem/EMD Chemicals (San Diego, CA). Silicon wafers were purchased from Silicon Quest (Reno, NV). Ultrapure water (UP H_2O) (resistivity = 18.3 MΩ cm; total organic content of 5 ppb) was obtained from a NANOpure Infinity System from Barnstead (Dubuque, IA).

2.2. Synthesis and Characterization of Polysarcosine Brush Polymers (PSAR). Polysarcosine of various chain lengths (PSAR-*n*) with the DOPA-Lys pentapeptide surface grafting anchor was synthesized using the solid-phase synthesis protocol described for our previously introduced peptoid antifouling brushes.[40,41,43] Briefly, the C-terminal DOPA-Lys-DOPA-Lys-DOPA pentapeptide surface anchor was first synthesized on a rink amide resin using conventional Fmoc solid-phase peptide synthesis (SPPS);[52] the polypeptoid portion was then coupled using the conventional submonomer protocol.[53] Methylamine, dissolved in tetrahydrofuran at 2 M (commercially sourced) and diluted in an equal volume of *N*-methylpyrrolidone, was used as the sarcosine side chain submonomer. Pure polysarcosine peptoids without the DOPA-Lys anchor (20-mers) were also synthesized by initiating the submonomer protocol directly on the resin. For comparison purposes, the peptide analogue polyalanine (20-mers) was synthesized by standard Fmoc SPPS initiated directly on the resin. The N-termini of all peptoid/peptide chains were acetylated with 1 M acetic anhydride in DCM for 30 min. All reactions were carried out on a C S Bio 036 automated peptide synthesizer (C S Bio, Menlo Park, CA). Cleavage from the resin and deprotection of all of the polymers were accomplished by standard 95% TFA treatment. The crude products were purified by diethyl ether precipitation and preparative RP-HPLC. The purity of the final products was confirmed by analytical RP-HPLC and MALDI-MS. All HPLC measurements were performed on a Waters system (Waters, Milford, MA) using Vydac C18 columns.

2.3. Preparation of PSAR Brush Surfaces on TiO_2 Surfaces. 3.5 nm thick TiO_2 native oxide films were deposited on Si wafers by electron beam evaporation (Edwards Auto500; 6×10^{-6} Torr, 0.1 nm/s) as previously demonstrated.[43] The TiO_2 wafers were cleaved into 11 × 12 mm^2 samples and individually marked for measurements. The substrates were cleaned by sonication in successive water, acetone, and 2-propanol baths and dried under N_2, and then by a reactive O_2 plasma (120 mTorr, 100 W, 3 min; Harrick Scientific, Ossining, NY). PSAR-*n* brushes were then grafted by immersing the TiO_2 samples in PSAR-*n* solutions (3 M NaCl buffered with 0.1 M MOPS, pH 6, 60 °C) at different concentrations and durations to obtain a range of grafted chain densities. All wafers within a batch of preparation were placed face up in sealed cell culture flasks, and the coating solution was constantly swirled within a heated orbital shaker. After being coated, the substrates were extensively rinsed with UP H_2O and dried in a stream of filtered N_2.

Sterile PSAR-20 brush surfaces were used for the cell culture experiments. The O_2 plasma cleaned TiO_2 samples were transferred into a sterile cell culture hood and placed on sterilized tissue soaked in 70% ethanol to sterilize the substrate backside, and irradiated with UV light of the cell culture hood for at least 30 min to sterilize also the top side. The sterilized substrates were then placed in sterile 12.5 cl flasks, and coated with PSAR solutions that were filter sterilized using 0.2 μm filter membranes. The coated samples were rinsed with sterilized water inside the cell culture hood before being placed at the bottom of sterile 24-well plates for cell culture.

2.4. PSAR Brush Density Characterization. The dry brush thickness (d) of each sample was measured by spectroscopic ellipsometry (M-2000, J.A. Woollam, Lincoln, NE), and the grafted chain density (σ) was calculated from the thickness values: $\sigma = N_A \rho d / M_w$, where N_A is Avogadro's number, ρ is the surface mass density, and M_w is the molecular weight. Ellipsometry spectra (377−1000 nm) were analyzed with a multilayer optical model. The refractive index ($n_{PSAR}(\lambda) = 1.503 + 0.006/\lambda^2$) of polysarcosine was measured from thick spin-coated polysarcosine films using a previously described protocol.[43] The mass densities of PSAR-10 and PSAR-20 ($\rho_{PSAR=10}$ and $\rho_{PSAR=20}$) were calculated by dividing their M_w (precisely known for the monodisperse solid-phase synthesized polymers) by their molecular volumes (obtained from atomistic models of the polymers; see the Supporting Information), $\rho_{PSAR=10}$ = 1.46 g/cm^3 and $\rho_{PSAR=20}$ = 1.42 g/cm^3. Atomistic model values were also verified by comparison of the model sarcosine monomer volume with experimental measurements using the aforementioned protocol on spin-coated films; both methods yielded a sarcosine monomer volume of 0.09 nm^3.

2.5. Contact Angle Measurements. Advancing and receding water contact angles were measured using the dynamic sessile drop

dx.doi.org/10.1021/la302131n | *Langmuir* 2012, 28, 16099−16107

method with a contact angle goniometer fitted with a high-frame-rate video camera and an automated pipet (model 190 CA, Ramé-Hart, Succasunna, NJ). To begin the measurement, a 1 μL UP H_2O drop was first placed on the substrate, and the tip of the automated pipet was lowered into the drop just behind the drop apex (to minimize distortion of the drop shape from the viewpoint of the camera). Water was supplied to the drop in steps of 0.08 μL at ~2 Hz. The contact angles were determined by automated, live video image analysis of the expanding water drop in profile (DropImage, Ramé-Hart, Succasunna, NJ). At the end of the advancing sequence, the drop volume was ~7 μL, the pipet tip was immediately withdrawn, and an image of the drop was saved as a record (within ~1 s after the drop has stopped moving). The same procedure was applied to record the receding angle: the pipet tip was lowered back into position, and water was withdrawn, also in steps of 0.08 μL at ~2 Hz.

2.6. Protein Adsorption Measurements. Lyophilized human fibrinogen (Fg; Sigma, Milwaukee, WI) was dissolved in pH 7.4, 10 mM hepes buffer, 150 mM NaCl at a concentration of 3 mg/mL. The normal physiological concentration of fibrinogen is between 2 and 4 mg/mL. Each PSAR coated TiO_2 sample was cleaved in half, with the experimental half-sample placed in protein solution and the control half placed in unloaded buffer. The samples were incubated at 37 °C for 20 min or 18 h and then rinsed in UP H_2O, and dried under a stream of N_2. The amount of adsorbed proteins was obtained from ellipsometer measurements in air of the adlayer thickness relative to the peptoid brush thickness of the control immersed in unloaded buffer (assuming $n = 1.45 + 0.01/\lambda^2$; $N = 3$; previous measurements showed that a mass density of 521 ng/cm^2 corresponded to a 3.7 nm Fg layer adsorbed on uncoated TiO_2[42]). Note that the present measurement approach with a rinsing step might only measure the majority fraction of fibrinogen that is irreversibly adsorbed on fouling surfaces, as judged by in situ measurements.[54] The fraction of reversibly bound proteins may be important components of the protein adsorption process for certain biological responses related to protein adsorption.[5,54,55] On the other hand, in situ measurements have shown that, after a transient adsorption spike upon injection of protein solution, antifouling PEG brushes (although not OEG SAMs)[51,56] can resist fibrinogen adsorption essentially to the same extent before as after rinsing,[57,58] and we expect a similar behavior on the present PSAR brushes. The drying step also likely introduced significant conformational changes to the adsorbed fibrinogen. Notwithstanding, our ex situ protocol has been validated by comparison with in situ measurements in terms of the protein mass adsorbed,[42,59,60] and the present results are expected to represent the amount of fibrinogen adsorption well.

2.7. Mammalian Cell Attachment Assay. Swiss albino 3T3 fibroblasts (CCL-92, ATCC, Manassas, VA) were cultured with Dulbecco's Modified Eagles media incorporating 10% calf bovine serum (CBS) and 1% penicillin-streptomycin (PS) solution following standard ATCC protocol. They were harvested using 0.25% trypsin-EDTA and counted using a hemocytometer immediately before use. Cells were seeded on PSAR-20 brush coated TiO_2 and on uncoated TiO_2 controls placed in 24-well plates at a density of 5000 cells/well ($N = 3$). At specified time points, the cell suspension was exchanged with 4 μM calcein AM dissolved in phosphate buffered saline (20 min incubation at 37 °C) to stain (30 min) for live, surface-attached fibroblasts. The substrates were then transferred to new culture plates with fresh buffer and imaged with an epifluorescence microscope while being immersed in solution. After imaging, substrates were reseeded with fresh cells in the standard DMEM/CBS/PS media and placed back into the incubator; media were changed every 3 days. The samples were reseeded after imaging, or at least twice weekly, whichever was sooner. The cell-covered surface area was quantified by image analysis (three images per substrate).

2.8. Bacterial Attachment Assay. *Escherichia coli* (ATCC 35218) glycerol stock was streaked on LB agar plates, and *Staphylococcus epidermidis* (RP62A) and *Pseudomonas aeruginosa* (ATCC 27853) glycerol stocks were streaked on tryptic-soy agar plates for overnight culture at 37 °C. To generate stock cultures, 3–4 colonies were transferred to LB broth for *E. coli* and tryptic-soy broth for *S. epidermidis* and *P. aeruginosa*. Following overnight incubation at 37 °C, approximate CFU counts were computed on the basis of absorbances (at 600 nm) from previously established growth curves. To prepare the inocula, cells were centrifuged at 10 000 rpm at 4 °C, and the obtained pellets were resuspended in sterile 0.85% NaCl solution. Subcultures of the inocula were performed to confirm cell concentrations to be within a log unit of 1×10^8 CFU/mL.

Dynamic attachment assays were performed using *E. coli* and *P. aeruginosa* to mimic the surface flow conditions in biomedical catheters. Sample substrates were placed into a 70 mL flat-bottom tissue culture flask, covered with 5 mL of the inoculum solution, and placed on an oscillating stage (60 rpm). Static attachment assays were performed using *S. epidermidis*, a strain which avoids surface-attachment under shear.[61] Samples for *S. epidermidis* were placed into wells of a 24-well tissue culture plate and covered with 1 mL of the inoculum solution. All samples were then incubated for 24 h at 37 °C ($N = 3$). Afterward, the inoculum solutions were exchanged with 0.85% NaCl solution ("rinsing"), stained with a live/dead stain (Syto-9/Propidium-Iodide) for 15 min, rinsed again with 0.85% NaCl, and mounted on glass microscope slides using mounting medium. The relative area covered by cells was determined using ImageJ.

2.9. Molecular Theory. The calculation details have been described in previous publications.[26,42,43,62] The basic idea is to consider conformations of the grafted polymer molecules and proteins. By minimization of the system's free energy, the probability of each of those conformations is determined depending on the solution conditions. This enables the investigation of both structural and thermodynamic properties of the equilibrium state of the explicit molecular system studied, for the complete range of surface coverages from very dilute (mushroom), to intermediate, and to highly stretched (brush) regimes. In applying the molecular theory to PSAR peptoid brushes, the polymer was considered to have one large headgroup representing the DOPA-Lys pentapeptide anchor (volume = 0.3 nm^3 and binding energy with TiO_2 = $-84\ k_BT$, as described in ref 43), and multiple smaller sarcosine monomer segments (volume = 0.09 nm^3; see section 2.3). Fibrinogen was modeled as a molecule composed of three spheres, which represents the three-lobed elongated structure of the actual protein, and was based on previous success in predicting experimental observations.[29,43,63] In accordance with the experimental observations of the present study, the polymer–polymer and polymer–protein interaction strengths were taken to be $-50/T$ and $-170/T$, respectively.

3. RESULTS AND DISCUSSION

3.1. Characterization of Polysarcosine Polymer Brushes (PSAR-*n*). The chemical structure of the PSAR-*n* brush molecule is shown in Scheme 1. Polysarcosine chain lengths of $n = 10$ and 20 sarcosine units were studied experimentally. Solid-phase synthesis and HPLC were used to obtain monodisperse polymers for comparison with molecular theory. The polymers were grafted onto TiO_2 substrates using a DOPA-Lys pentapeptide surface-grafting anchor (DOPA = 3,4-dihydroxy-phenylalanine and Lys = lysine) inspired by mussel adhesive proteins.[40,43] DOPA and Lys amino acids are found enriched in the adhesive plaques that marine mussels use to attach strongly on a variety of wet surfaces.[64,65] As many biomedical implants make use of titanium alloys,[10] TiO_2 was chosen as a model substrate. As previously demonstrated,[40,43] the use of the DOPA-Lys anchor not only enables secure grafting of a peptoid brush monolayer onto TiO_2 substrates, but also the convenient control of the brush grafting density by a solution grafting-to approach.

Figure 1 illustrates, using PSAR-20 as an example, that the grafted chain density can be controlled across a wide range. Higher deposition concentrations and longer deposition durations promoted the insertion and accommodation of PSAR chains at higher surface densities within the peptoid

dx.doi.org/10.1021/la302131n | Langmuir 2012, 28, 16099–16107

Scheme 1. Chemical Structure of the Polysarcosine Peptoid with DOPA-Lys Surface-Anchoring Pentapeptide (PSAR-*n*), as well as the Structures of the Pure Polysarcosine 20-mer (SAR-20) and Polyalanine 20-mer (Ala-20)

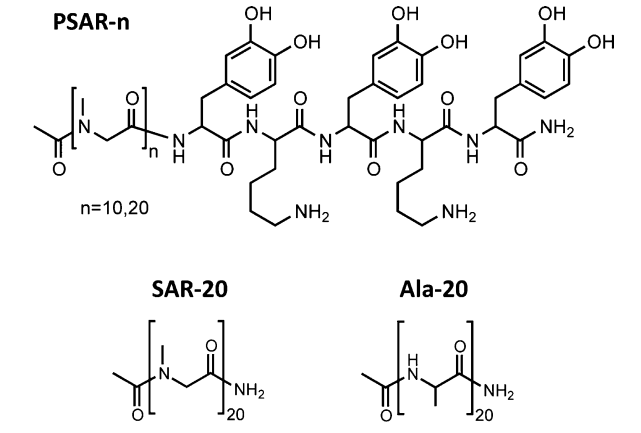

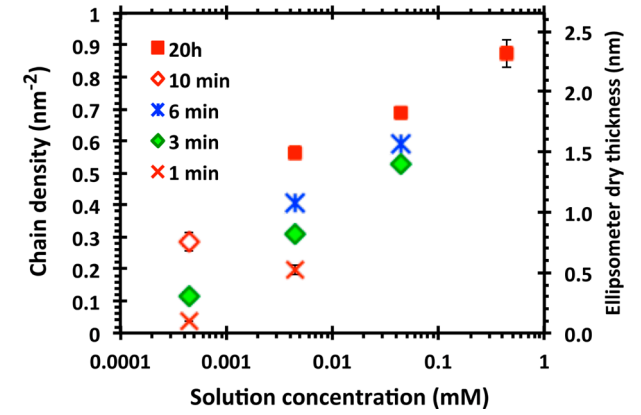

Figure 1. The surface density of grafted PSAR-20 chains (left axis) and the corresponding brush thickness in the dry state as measured by ellipsometry (right axis). A wide range of surface chain densities was achieved by solution grafting of PSAR-20 from varying solution concentrations and durations of exposure. The error bars indicate ±1 SD.

layer. Further, to promote monolayer grafting, the depositions were performed at pH 6 to prevent the catechol cross-linking and polymerization that is observed at basic pH, and which give rise to disordered coatings of greater thickness.[65,66] The highest PSAR-20 density achieved was 0.87 nm^{-2}, corresponding to a dry brush thickness of 2.3 nm and an average chain separation of 1.2 nm (assuming a close-packed array of the DOPA-Lys anchors). For PSAR-10, the highest chain density achieved was 0.95 nm^{-2} (dry thickness = 1.7 nm and average chain separation = 1.1 nm). This range of chain separations (1.1−1.2 nm) is similar to the estimated footprint diameter of the DOPA-Lys pentapeptide segment,[67] and chain densities could not be increased significantly further within a monolayer.

The solution-phase behavior of grafted polysarcosine was also investigated with liquid AFM measurements (see the Supporting Information). AFM imaging showed a smooth PSAR-20 surface when grafted at 0.82 nm^{-2} and did not reveal any obvious defects in the brush layer. AFM contact mode "scratching" experiments also revealed a wet thickness of ∼6 nm for the 0.82 nm^{-2} PSAR-20 brush (dry thickness = 2.2 nm). The contour length of the polysarcosine 20-mer is 6.8 nm, and that of the DOPA-Lys pentapeptide anchor is 1.7 nm (using the value of 0.34 nm per residue for amino acids). The absolute thickness of the PSAR-20 layer is difficult to measure because the height position of the (dynamic) polymer brush depends on the force applied by the AFM tip during imaging, and because AFM scratching cannot guarantee that all of the polymer material has been displaced with the AFM tip.

To obtain insight into the hydrophilicity of the PSAR brush, the water wetting behavior of the grafted PSAR brush and the partitioning of the standalone polysarcosine peptoid in water were characterized. Figure 2 shows that the advancing water

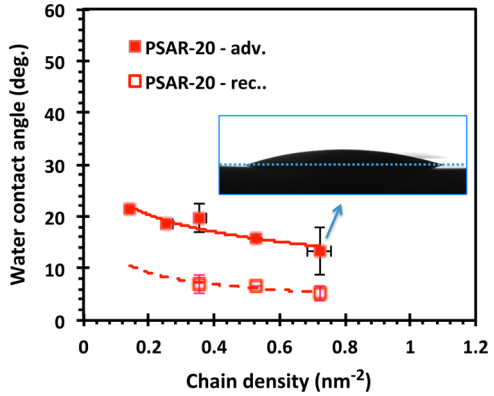

Figure 2. The advancing and receding water contact angles recorded on PSAR-20 surfaces with a range of different grafted chain densities. The inset shows the optical image of a 7 μL water drop in profile, at the end of an advancing contact angle measurement (see Experimental Section), and illustrates the low water contact angles a polysarcosine brush surface makes at high chain densities. The error bars indicate ±1 SD.

contact angle measured on PSAR-20 was reduced by increasing the density of the polysarcosine chains from >20° at low brush densities to a minimum of 13° at high densities. In contrast, the advancing angle of a homogeneous layer of the DOPA-Lys anchor without the peptoid segment was measured at 39°.[43] The advancing contact angle measured on PSAR-10 at the highest chain densities was 33° (see the Supporting Information) and likely indicated the influence of the underlying DOPA-Lys anchor layer. Receding contact angle measurements revealed that both PSAR-10 and PSAR-20 brushes at all chain densities were nearly completely wetted (θ_{rec} = 5−7°) and suggested the strong interaction of the polysarcosine peptoid with water.

The observations above were corroborated by RP-HPLC measurements of the standalone 20-mer polysarcosine peptoid (i.e., without the DOPA-Lys anchor) using a water−acetonitrile (ACN) gradient (Figure 3). A C_{18} alkyl-chain-modified column was used to probe the relative hydrophobic interactions of the test molecules between the column material and a range of water−ACN solvent compositions. More hydrophobic and/or larger molecules interact more strongly with the column and elute only with a less hydrophilic solvent (i.e., higher ACN content in the present measurement). As shown in Figure 3, the pure polysarcosine 20-mer eluted at 81% water (19% ACN), and the longer PSAR-20 with both the polysarcosine and the DOPA-Lys pentapeptide eluted at 78% water (22% ACN). In comparison, the much shorter DOPA-Lys pentapeptide eluted at only a slightly higher 84% water (16% ACN), while a pure polyalanine 20-mer peptide eluted at a much lower 63% water (37% ACN). Thus, the elution of PSAR species at

dx.doi.org/10.1021/la302131n | *Langmuir* 2012, 28, 16099−16107

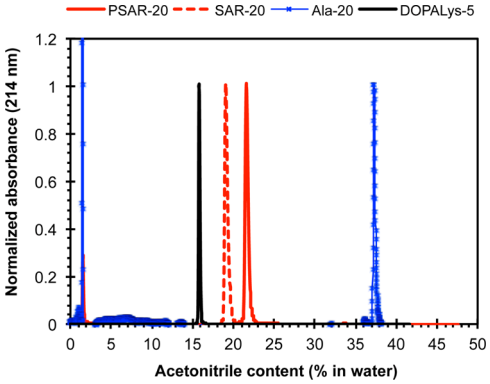

Figure 3. RP-HPLC elution of the pure polysarcosine (SAR-20), pure polyalanine (Ala-20), the standalone DOPA-Lys pentapeptide anchor (DOPALys-5), and the PSAR-20 brush molecule using an analytical C18 column. The HPLC gradient used was an increase of 1% ACN/min starting at 2% ACN in water with 0.1% added TFA. The UV absorbances of the amide moieties along the peptoid/peptide backbone (at 214 nm) were background subtracted and normalized for comparison. The disturbance at 2 min was the injection peak.

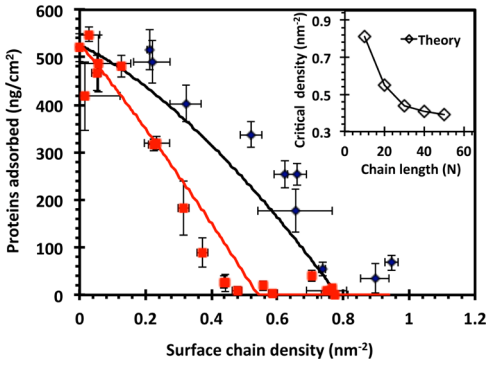

Figure 4. The amount of irreversibly adsorbed fibrinogen as a function of PSAR surface chain density. "◆" represent experiment data for PSAR-10; the black line shows the corresponding adsorption behavior predicted by molecular theory. Red "■" represent experiment data for PSAR-20; the red line shows the corresponding theoretical prediction. The experiments were performed with 3 mg/mL fibrinogen in HEPES buffer at 37 °C. The experimental critical chain densities for inhibiting fibrinogen adsorption are ~0.5 nm^{-2} for PSAR-20 and ~1 nm^{-2} for PSAR-10. The error bars represent ±1 SD. The inset shows the theoretical critical chain densities for chain lengths = 10 and 20, as well as for an extended range of chain lengths up to 50-mers for which experimental data are not available.

relatively high water contents indicates a relatively strong interaction of polysarcosine with water. This is consistent with observations that discrete sarcosine substitutions along model polypeptide sequences are more hydrophilic than alanine and even lysine residue.[46] Although a low water contact angle is not required for good antifouling behavior (e.g., nonfouling PEG brush surfaces exhibit contact angles typically in the range of 30−40°), the water contact angle and HPLC data (Figures 2 and 3) do indicate a strong interaction of polysarcosine with water, which could benefit antifouling performance.[2]

3.2. Protein Adsorption on PSAR Brushes. As a biomaterial comes into contact with body fluids, the process of protein adsorption occurs rapidly and the adsorbed proteins may mediate subsequent cell interactions.[2,11] The resistance against protein adsorption is therefore one indication of the performance of an antifouling surface. Fibrinogen (Fg) was chosen as a model protein to probe the resistance of PSAR brushes against protein adsorption because the molecular theory for Fg is already well developed.[29,43,63] Furthermore, Fg is an important protein in platelet and monocyte adhesion, in the coagulation pathway, and in inflammation.[3,68] (However, other plasma proteins may play a higher regulatory role.[5,68]) Fg adsorption data on a range of antifouling polymer brushes, including PEG, have also been reported and are compared to the present polysarcosine system in the Supporting Information.

PSAR brushes were prepared at a range of chain densities and challenged with Fg solutions (3 mg/mL, the average concentration in blood plasma). As seen in Figure 4, the amount of proteins adsorbed decreased monotonically with increasing chain density, likely because protein insertion into the tethered peptoid layer is increasingly prevented by the excluded volume repulsions of a larger number of grafted chains, as well as the decreasing entropic degrees of freedom of the chains if a protein was inserted.[26] (Note that the present measurement approach with a rinsing step only measured the majority fraction[54] of fibrinogen that is irreversibly adsorbed on the surface.)

Furthermore, it was observed that short-term fibrinogen adsorption was essentially inhibited above the "critical" densities of ~0.5 nm^{-2} for PSAR-20 and approximately 1 nm^{-2} for PSAR-10. We have previously shown that the critical density to preventing protein adsorption is an important parameter to quantitatively characterize the antifouling performance of surface-grafted polymer brushes.[43] By this measure, the brushes composed of PSAR are comparable to the performance of our previously introduced peptoid with PEG-mimetic side chains (critical density ~0.5 nm^{-2}),[43] and also that of conventional PEG of similar molecular weight.[69,70] A comparison of fibrinogen adsorption as a function of chain density on PSAR-20 with literature data concerning surface-grafted PEG and acrylate polymers with oligo(ethylene glycol) and with phosphorylcholine side chains is included in the Supporting Information.

The experimental data in Figure 4 actually consist of results from both 20 min and 18 h experiments. Consistent, albeit slight, decreases in the polysarcosine chain densities were measured from control samples after extended immersion of the brush coated substrates in protein solution, and the chain densities plotted in Figure 4 correspond to these final values. However, no obvious difference in the trends of protein adsorption versus chain density was observed between the 20 min and 18 h sample sets (separate data not shown). We also note that the current fibrinogen adsorption measurements were performed under static conditions and involved sample rinsing, and hence were designed only to illustrate the potential of PSAR surfaces to resist protein adsorption instead of as an explicit model of blood plasma−surface interactions.

The increasing ability of the PSAR brushes to inhibit protein adsorption at higher chain densities is generally reproduced by the molecular theory, shown also in Figure 4 (solid curves). In particular, a longer chain is able to inhibit protein adsorption at a lower chain density because a relatively higher density of polymer segments is maintained even at a lower chain density for longer chains, and because the time required for an initial adsorption event is predicted to grow rapidly with the chain length.[28] This effect is illustrated in the inset of Figure 4, which plots the critical densities predicted by molecular theory for completely preventing fibrinogen adsorption over an extended

dx.doi.org/10.1021/la302131n | Langmuir 2012, 28, 16099−16107

range of PSAR chain length. It is seen that the marginal reduction in chain density required to inhibit protein adsorption (i.e., the "improvement" in antifouling performance for increasing the chain length) decreases rapidly with increasing chain length. Specifically, the molecular theory predicts that a shift from PSAR-10 to PSAR-20 would provide more than half of the potential improvement toward the long chain length limit (the predicted critical chain density at a chain length of 50 monomers is 0.39 chain/nm^2, and appears to approach the asymptotic value). Indeed, the present protein adsorption experimental results indicate that the use of PSAR-20 instead of PSAR-10 dramatically decreased the critical chain density from ~1 to ~0.5 nm^{-2}. The molecular theory applied has also been corroborated by experimental observations of protein adsorption on PEG and other peptoid brushes.[29,43,63] Knowledge of the critical density behavior for an antifouling polymer brush system is important because grafting longer polymer chains at higher densities can be increasingly inconvenient (e.g., in requiring longer processing conditions and/or larger amounts of polymer material; see Figure 1).

3.3. Prevention of Mammalian Cell and Bacterial Attachment. On the basis of the excellent resistance of the PSAR-20 brush against protein adsorption, evaluation of the PSAR system against cell attachment focused on this 20-mer chain length. PSAR-20 brush coated surfaces were challenged by the long-term culture of mouse fibroblasts (3T3-Swiss albino) to evaluate the antifouling performance against mammalian cell attachment. Although not directly related to surface-induced thrombosis and hemocompatibility, fibroblasts are responsible in another important area of biocompatibility; the synthesis of collagen during fibrous encapsulation and their proliferation lead to the formation of granulation tissue.[11] The extents of fibroblast attachment on PSAR-20 as well as on the uncoated TiO_2 control are compared in Figure 5A. An initial PSAR chain density of 0.87 nm^{-2}, above the critical density to prevent fibrinogen adsorption, was chosen for these experiments. Consistent with the inhibition of protein adsorption at high chain densities, it is seen that fibroblast attachment on PSAR-20 was severely limited. The number of attached fibroblasts, stained green by calcein AM (Figure 5B) and represented by the total cell surface coverage (Figure 5A), was maintained at a very low level (≤1%) over the prolonged experimental time frame (7 weeks). In contrast, fibroblasts proliferated on uncoated TiO_2 controls and attained full coverage (corresponding to 5 × 10^4 cell/cm^2) 1 week after initial cell seeding. Fibroblasts require an attachment surface to survive and proliferate. However, they were unable to do so on PSAR-20, and the still suspended cells were removed during media exchange for the cell-staining procedure. To test for long-term antifouling effectiveness, new cells were seeded twice a week to continuously challenge the PSAR-20 surface. For the small number of cells that remained on the PSAR-20 surface at each time point, all exhibited a rounded morphology and extended no or very few filopodia (Figure 5B), indicating that the cells were very limited in their ability to interact with the antifouling surface. In contrast, the fibroblasts spread very well on the uncoated TiO_2 surface. A comparison of long-term fibroblast attachment on PSAR-20 with literature data for surface-grafted PEG and acrylate polymers with oligo(ethylene glycol) and with sulfobetaine side chains is included in the Supporting Information.

Although we were unable to correlate protein adsorption with the cell culture data throughout the 7 wk experimental

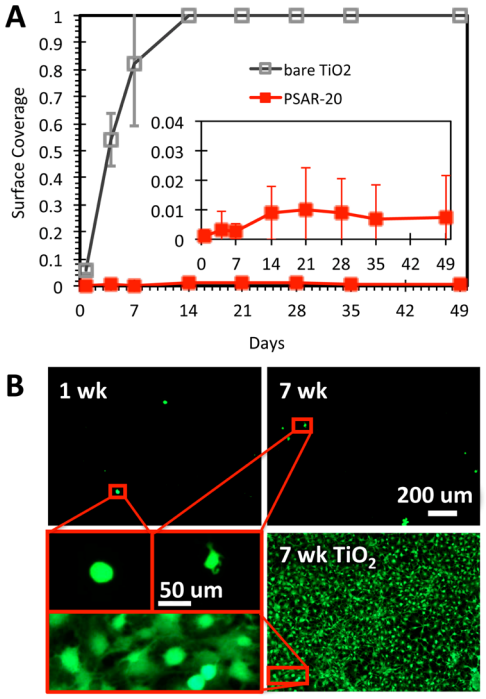

Figure 5. The resistance of the PSAR-20 brush surface (chain density = 0.87 nm^{-2}) against 3T3 mouse fibroblast attachment. The cells were stained with calcein AM. Part (A) plots the surface coverage of fibroblasts observed on the PSAR-20 brush over 49 d (7 weeks). Fresh fibroblasts were reseeded on the samples twice a week. The number of cells attached on PSAR-20 was very low throughout, while a confluent layer (coverage = 1) was achieved on the uncoated TiO_2 control surface after 7 d. Although some cells were observed on the PSAR-20 surface, part (B) shows that their morphologies were rounded, exhibiting few filopodia, and were poorly attached. In contrast, cells on the TiO_2 control spread very well and formed a confluent cell sheet after 1 week of cell culture (A). The error bars indicate ±1 SD.

period, we were able to measure, over the course of 8 d, the amount of protein adsorption from the cell culture media (incorporating 10% bovine serum) on control PSAR-20 substrates (see the Supporting Information). It was observed that 20−40 ng/cm^2 of material was adsorbed on PSAR-20 substrates after overnight immersion in the cell culture media, but that the amount of adsorbed matter stayed relatively constant up to 8 d. In contrast, the amount adsorbed on TiO_2 control substrates was 570 ng/cm^2 on day 8. Therefore, the adsorption of 20−40 ng/cm^2 of cell culture media on PSAR-20 was not able to support fibroblast attachment within the first week of experiments, and this relatively low level of adsorption might also be correlated to the long-term inability of fibroblasts to attach on PSAR-20.

The resistance against bacterial attachment was also evaluated (Figure 6). Two Gram-negative strains, *Pseudomonas aeruginosa* and *Escherichia coli*, and a Gram-positive strain, *Staphylococcus epidermidis*, were selected due to biofilm-forming behavior and prevalence in medical device-related infections. Both Gram-positive and Gram-negative bacteria can be found as part of an infectious biomass associated with pneumonia, and urinary tract, surgical site, and bloodstream infections.[12,13] While *P. aeruginosa* only accounts for approximately 11% of nosocomial infection pathogens, pseudomonal pneumonia is often associated with high morbidity, with 70−90% mortality reported.[71,72]

dx.doi.org/10.1021/la302131n | *Langmuir* 2012, 28, 16099−16107

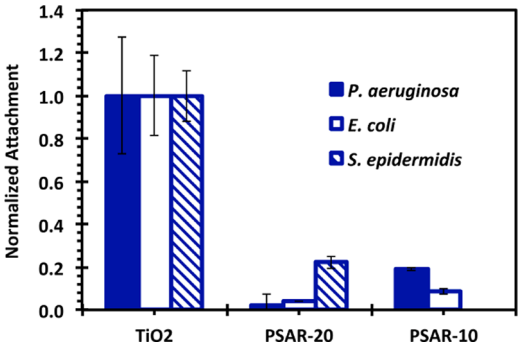

Figure 6. The ability of PSAR-10 and PSAR-20 brushes to resist attachment of bacteria over 24 h. *Pseudomonas aeruginosa* was seeded at 3×10^7 CFU/mL, and *Escherichia coli* was seeded at 6×10^8 CFU/mL. *Staphylococcus epidermidis* was seeded at 4×10^7 CFU/mL. The PSAR-20 chain density was 0.87 nm^{-2}, and the PSAR-10 chain density was 0.95 nm^{-2}. Seeding of *S. epidermidis* was not performed on PSAR-10. Normalization is performed for data obtained for measurements of each specific bacterial strain. For a given strain, the seeding density is maintained between all sample conditions tested. The normalized data are specific to individual species and not between all three strains. The error bars indicate ±1 SD.

In these experiments, the samples were rinsed for bacterial staining, and only the surface-attached bacterial cells were counted. As a surface with no antimicrobial activity that resists attachment only by physicochemical means, the PSAR-20 brush was found to be quite effective against the attachment of both *P. aeruginosa* and *E. coli*. Attachments of these two strains were reduced by >95% as compared to the uncoated TiO_2 control. Incidentally, conventional PEG is known to be relatively ineffective against *P. aeruginosa* attachment.[73] PSAR-20 was also significantly more effective than PSAR-10 at resisting the attachment of these two Gram-negative strains. However, a small but significant amount of *S. epidermidis* attached on the PSAR-20 brush (~80% reduction). The performance of PSAR-10 against *S. epidermidis* attachment was expected to be lower and was not tested. Notwithstanding, based on the protein adsorption results and the reduced attachment of *P. aeruginosa* and *E. coli* on PSAR-20 as opposed to PSAR-10, PSAR brushes at longer chain lengths may further inhibit the attachment of all of the bacterial strains tested.

4. CONCLUSIONS

Polysarcosine, the elementary poly(N-substituted glycine) peptoid, was demonstrated to be an excellent antifouling polymer when surface grafted as a polymer brush. Polysarcosine brushes (PSAR-*n*) were surface grafted on TiO_2 by a mussel-adhesive-inspired DOPA-Lys pentapeptide. This grafting strategy enabled fine control over the surface chain densities over a wide range. At high chain densities, the grafted PSAR-20 brushes exhibited very low water contact angles, and HPLC measurements showed that standalone polysarcosine is much more hydrophilic than its peptide analogue, polyalanine. These measurements indicated that the polysarcosine peptoid backbone possesses a strong and favorable interaction with water. The control over grafting densities also allowed the identification of the critical chain densities above which PSAR-10 (1 nm^{-2}) and PSAR-20 (0.5 nm^{-2}) can effectively inhibit fibrinogen adsorption. Molecular theory calculations of fibrinogen adsorption on the PSAR-*n* brushes corresponded well with the experimental data, and showed that the critical chain density could be further reduced at longer PSAR chain lengths. Moreover, the good predictive power of the theory reinforces the idea that the main mechanism for preventing protein adsorption by the polypeptoid brush is due to steric repulsions, that is, the restriction on the number of peptoid conformations and the high local osmotic pressure that results from protein insertion into the peptoid layer.

Consistent with the high resistance against protein adsorption, PSAR-20 at a high brush density was demonstrated to resist mammalian cell (mouse fibroblast) attachment over an extended period of 7 weeks while being challenged with repeated seeding with fresh cells. This suggests polysarcosine brush coatings could prevent undesirable protein adsorption and cell attachment. The PSAR-20 brushes were also shown to resist the attachment of both *E. coli* and *P. aeruginosa*. In addition to the excellent antifouling properties demonstrated, polypeptoid have been shown to resist proteolytic degradation,[21,24,25] and polysarcosine can be produced in large quantities by *N*-carboxy anhydride polymerization.[45,49] In summary, surface-grafted polysarcosine peptoid brushes hold great promise as an antifouling design for biomedical applications.

■ ASSOCIATED CONTENT

Supporting Information

(i) The molecular volumes of PSAR molecules; (ii) water contact angle data for PSAR-10; (iii) a comparison of protein adsorption on PSAR-20 with PEG, POEGMEMA, and zwitterionic MPC brushes; (iv) a comparison of long-term fibroblast attachment on PSAR-20 with PEG, POEGMEMA, and zwitterionic PSBMA brushes; (v) liquid AFM studies of the PSAR-20 brush layer; and (vi) medium-term adsorption of cell culture media material on PSAR-20. This material is available free of charge via the Internet at http://pubs.acs.org.

■ AUTHOR INFORMATION

Corresponding Author

*E-mail: igalsz@northwestern.edu (I.S.); philm@northwestern.edu (P.B.M.).

Notes

The authors declare no competing financial interest.

■ ACKNOWLEDGMENTS

This research was supported by grant number EB005772 from the National Institute of Biomedical Imaging and Bioengineering (NIBIB) at the National Institutes of Health (NIH). K.H.A.L. acknowledges support by fellowship number HL104966 from the National Heart, Blood and Lung Institute (NHBLI) at the NIH. C.R. acknowledges support by the National Natural Science Foundation of China under Grant 10974080. We thank Jinghao Kuang and Piotr Maniak for technical support. Profilometry and MALDI-MS were performed at KeckII/NUANCE and IMSERC, respectively, both at Northwestern University.

■ REFERENCES

(1) Sapatnekar, S.; Kieswetter, K. M.; Merritt, K.; Anderson, J. M.; Cahalan, L.; Verhoeven, M.; Hendriks, M.; Fouache, B.; Cahalan, P. Blood biomaterial interactions in a flow system in the presence of bacteria − Effect of protein adsorption. *J. Biomed. Mater. Res.* **1995**, *29*, 247−256.

(2) Ostuni, E.; Chapman, R. G.; Holmlin, R. E.; Takayama, S.; Whitesides, G. M. A survey of structure−property relationships of

surfaces that resist the adsorption of protein. *Langmuir* **2001**, *17*, 5605−5620.
(3) Kwak, D.; Wu, Y.; Horbett, T. A. Fibrinogen and von Willebrand's factor adsorption are both required for platelet adhesion from sheared suspensions to polyethylene preadsorbed with blood plasma. *J. Biomed. Mater. Res., Part A* **2005**, *74A*, 69−83.
(4) Arima, Y.; Kawagoe, M.; Toda, M.; Iwata, H. Complement activation by polymers carrying hydroxyl groups. *ACS Appl. Mater. Interfaces* **2009**, *1*, 2400−2407.
(5) Vogler, E. A.; Siedlecki, C. A. Contact activation of blood-plasma coagulation. *Biomaterials* **2009**, *30*, 1857−1869.
(6) Nonckreman, C. J.; Fleith, S.; Rouxhet, P. G.; Dupont-Gillain, C. C. Competitive adsorption of fibrinogen and albumin and blood platelet adhesion on surfaces modified with nanoparticles and/or PEO. *Colloids Surf., B* **2010**, *77*, 139−149.
(7) Zilla, P.; Bezuidenhout, D.; Human, P. Prosthetic vascular grafts: Wrong models, wrong questions and no healing. *Biomaterials* **2007**, *28*, 5009−5027.
(8) Jordan, S. W.; Chaikof, E. L. Novel thromboresistant materials. *J. Vasc. Surg.* **2007**, *45*, 104A−115A.
(9) Venkatraman, S.; Boey, F.; Lao, L. L. Implanted cardiovascular polymers: Natural, synthetic and bio-inspired. *Prog. Polym. Sci.* **2008**, *33*, 853−874.
(10) Ratner, B. A perspective on titanium biocompatibility. In *Titanium in Medicine: Material Science, Surface Science, Engineering, Biological Responses and Medical Applications*; Brunette, D. M., Tengvall, P., Thomsen, P., Textor, M., Eds.; Springer: Berlin and Heidelberg, 2000; pp 1−12.
(11) Anderson, J. M. Biological responses to materials. *Annu. Rev. Mater. Res.* **2001**, *31*, 81−110.
(12) Weinstein, R. A.; Gaynes, R.; Edwards, J. R.; System, N. N. I. S. Overview of nosocomial infections caused by Gram-negative bacilli. *Clin. Infect. Dis.* **2005**, *41*, 848−854.
(13) Ziebuhr, W.; Hennig, S.; Eckart, M.; Kränzler, H.; Batzilla, C.; Kozitskaya, S. Nosocomial infections by Staphylococcus epidermidis: how a commensal bacterium turns into a pathogen. *Int. J. Antimicrob. Agents* **2006**, *28*, 14−20.
(14) Kuijer, R.; Jansen, E. J. P.; Emans, P. J.; Bulstra, S. K.; Riesle, J.; Pieper, J.; Grainger, D. W.; Busscher, H. J. Assessing infection risk in implanted tissue-engineered devices. *Biomaterials* **2007**, *28*, 5148−5154.
(15) Walkey, C. D.; Chan, W. C. W. Understanding and controlling the interaction of nanomaterials with proteins in a physiological environment. *Chem. Soc. Rev.* **2012**, *41*, 2780−2799.
(16) Rastogi, A.; Nad, S.; Tanaka, M.; Mota, N. D.; Tague, M.; Baird, B. A.; Abrunifa, H. c. D.; Ober, C. K. Preventing nonspecific adsorption on polymer brush covered gold electrodes using a modified ATRP initiator. *Biomacromolecules* **2009**, *10*, 2750−2758.
(17) Eglin, D.; Mortisen, D.; Alini, M. Degradation of synthetic polymeric scaffolds for bone and cartilage tissue repairs. *Soft Matter* **2009**, *5*, 938−947.
(18) Chelmowski, R.; Köster, S. D.; Kerstan, A.; Prekelt, A.; Grunwald, C.; Winkler, T.; Metzler-Nolte, N.; Terfort, A.; Wöll, C. Peptide-based SAMs that resist the adsorption of proteins. *J. Am. Chem. Soc.* **2008**, *130*, 14952−14953.
(19) Kanoatov, M.; Krylov, S. N. DNA adsorption to the reservoir walls causing irreproducibility in studies of protein-DNA interactions by methods of kinetic capillary electrophoresis. *Anal. Chem.* **2011**, *83*, 8041−8045.
(20) Le, N. C. H.; Gubala, V.; Gandhiraman, R. P.; Daniels, S.; Williams, D. E. Evaluation of different nonspecific binding blocking agents deposited inside poly(methyl methacrylate) microfluidic flow-cells. *Langmuir* **2011**, *27*, 9043−9051.
(21) Simon, R. J.; Kania, R. S.; Zuckermann, R. N.; Huebner, V. D.; Jewell, D. A.; Banville, S.; Ng, S.; Wang, L.; Rosenberg, S.; Marlowe, C. K.; Spellmeyer, D. C.; Tan, R. Y.; Frankel, A. D.; Santi, D. V.; Cohen, F. E.; Bartlett, P. A. Peptoids − A modular approach to drug discovery. *Proc. Natl. Acad. Sci. U.S.A.* **1992**, *89*, 9367−9371.
(22) Kodadek, T.; Reddy, M. M.; Olivos, H. J.; Bachhawat-Sikder, K.; Alluri, P. G. Synthetic molecules as antibody replacements. *Acc. Chem. Res.* **2004**, *37*, 711−718.
(23) Horne, W. S. Peptide and peptoid foldamers in medicinal chemistry. *Expert Opin. Drug Discovery* **2011**, *6*, 1247−1262.
(24) Miller, S. M.; Simon, R. J.; Ng, S.; Zuckermann, R. N.; Kerr, J. M.; Moos, W. H. Comparison of the proteolytic susceptibilities of homologous L-amino acids, D-amino-acid, and N-substituted glycine peptide and peptoid oligomers. *Drug Dev. Res.* **1995**, *35*, 20−32.
(25) Sui, Q.; Borchardt, D.; Rabenstein, D. L. Kinetics and equilibria of cis/trans isomerization of backbone amide bonds in peptoids. *J. Am. Chem. Soc.* **2007**, *129*, 12042−12048.
(26) Szleifer, I. Protein adsorption on surfaces with grafted polymers: A theoretical approach. *Biophys. J.* **1997**, *72*, 595−612.
(27) Halperin, A. Polymer brushes that resist adsorption of model proteins − Design parameters. *Langmuir* **1999**, *15*, 2525−2533.
(28) Fang, F.; Satulovsky, J.; Szleifer, I. Kinetics of protein adsorption and desorption on surfaces with grafted polymers. *Biophys. J.* **2005**, *89*, 1516−1533.
(29) McPherson, T.; Kidane, A.; Szleifer, I.; Park, K. Prevention of protein adsorption by tethered poly(ethylene oxide) layers: Experiments and single-chain mean-field analysis. *Langmuir* **1998**, *14*, 176−186.
(30) Kingshott, P.; Thissen, H.; Griesser, H. J. Effects of cloud-point grafting, chain length, and density of PEG layers on competitive adsorption of ocular proteins. *Biomaterials* **2002**, *23*, 2043−2056.
(31) Pasche, S.; Vörös, J.; Griesser, H. J.; Spencer, N. D.; Textor, M. Effects of ionic strength and surface charge on protein adsorption at PEGylated surfaces. *J. Phys. Chem. B* **2005**, *109*, 17545−17552.
(32) Nakaya, T.; Li, Y.-J. Phospholipid polymers. *Prog. Polym. Sci.* **1999**, *24*, 143−181.
(33) West, S. L.; Salvage, J. P.; Lobb, E. J.; Armes, S. P.; Billingham, N. C.; Lewis, A. L.; Hanlon, G. W.; Lloyd, A. W. The biocompatibility of crosslinkable copolymer coatings containing sulfobetaines and phosphobetaines. *Biomaterials* **2004**, *25*, 1195−1204.
(34) Zhang, Z.; Zhang, M.; Chen, S.; Horbett, T. A.; Ratner, B. D.; Jiang, S. Blood compatibility of surfaces with superlow protein adsorption. *Biomaterials* **2008**, *29*, 4285−4291.
(35) Estephan, Z. G.; Schlenoff, P. S.; Schlenoff, J. B. Zwitteration as an alternative to PEGylation. *Langmuir* **2011**, *27*, 6794−6800.
(36) Toomey, R.; Tirrell, M. Functional polymer brushes in aqueous media from self-assembled and surface-initiated polymers. *Annu. Rev. Phys. Chem.* **2008**, *59*, 493−517.
(37) Ayres, N. Polymer brushes: Applications in biomaterials and nanotechnology. *Polym. Chem.* **2010**, *1*, 769−777.
(38) Feng, W.; Gao, X.; McClung, G.; Zhu, S. P.; Ishihara, K.; Brash, J. L. Methacrylate polymer layers bearing poly(ethylene oxide) and phosphorylcholine side chains as non-fouling surfaces: In vitro interactions with plasma proteins and platelets. *Acta Biomater.* **2011**, *7*, 3692−3699.
(39) Lin, S.; Zhang, B.; Skoumal, M. J.; Ramunno, B.; Li, X.; Wesdemiotis, C.; Liu, L.; Jia, L. Antifouling poly(*β*-peptoid)s. *Biomacromolecules* **2011**, *12*, 2573−2582.
(40) Statz, A. R.; Meagher, R. J.; Barron, A. E.; Messersmith, P. B. New peptidomimetic polymers for antifouling surfaces. *J. Am. Chem. Soc.* **2005**, *127*, 7972−7973.
(41) Statz, A. R.; Park, J. P.; Chongsiriwatana, N. P.; Barron, A. E.; Messersmith, P. B. Surface-immobilised antimicrobial peptoids. *Biofouling* **2008**, *24*, 439−448.
(42) Statz, A. R.; Kuang, J. H.; Ren, C. L.; Barron, A. E.; Szleifer, I.; Messersmith, P. B. Experimental and theoretical investigation of chain length and surface coverage on fouling of surface grafted polypeptoids. *Biointerphases* **2009**, *4*, FA22−FA32.
(43) Lau, K. H. A.; Ren, C.; Park, S. H.; Szleifer, I.; Messersmith, P. B. An experimental−theoretical analysis of protein adsorption on peptidomimetic polymer brushes. *Langmuir* **2012**, *28*, 2288−2298.
(44) Douy, A.; Gallot, B. Amphipathic block copolymers with two polypeptide blocks: Synthesis and structural study of poly(N*ε*-

trifluoroacetyl-l-lysine)-polysarcosine copolymers. *Polymer* **1987**, *28*, 147−154.
(45) Fetsch, C.; Grossmann, A.; Holz, L.; Nawroth, J. F.; Luxenhofer, R. Polypeptoids from N-substituted glycine N-carboxyanhydrides: Hydrophilic, hydrophobic, and amphiphilic polymers with Poisson distribution. *Macromolecules* **2011**, *44*, 6746−6758.
(46) Tang, Y. C.; Deber, C. M. Hydrophobicity and helicity of membrane-interactive peptides containing peptoid residues. *Biopolymers* **2002**, *65*, 254−262.
(47) Bovey, F. A.; Ryan, J. J.; Hood, F. P. Polymer nuclear magnetic resonance spectroscopy. XV. The conformation of polysarcosine. *Macromolecules* **1968**, *1*, 305−307.
(48) Mattice, W. L. Comparison of conformational map for poly(L-proline) with conformational maps for polysarcosine and poly(N-methyl-L-alanine). *Macromolecules* **1973**, *6*, 855−858.
(49) Sisido, M.; Imanishi, Y.; Higashimura, T. Static and dynamic studies on the end-to-end intrachain energy transfer on a polysarcosine chain. *Macromolecules* **1979**, *12*, 975−980.
(50) Butterfoss, G. L.; Renfrew, P. D.; Kuhlman, B.; Kirshenbaum, K.; Bonneau, R. A preliminary survey of the peptoid folding landscape. *J. Am. Chem. Soc.* **2009**, *131*, 16798−16807.
(51) Ostuni, E.; Chapman, R. G.; Liang, M. N.; Meluleni, G.; Pier, G.; Ingber, D. E.; Whitesides, G. M. Self-assembled monolayers that resist the adsorption of proteins and the adhesion of bacterial and mammalian cells. *Langmuir* **2001**, *17*, 6336−6343.
(52) Chan, W. C.; White, P. D. *Fmoc Solid Phase Peptide Synthesis: A Practical Approach*; Oxford University Press: New York, 2000.
(53) Zuckermann, R. N.; Kerr, J. M.; Kent, S. B. H.; Moos, W. H. Efficient method for the preparation of peptoids [oligo(N-substituted glycines)] by submonomer solid-phase synthesis. *J. Am. Chem. Soc.* **1992**, *114*, 10646−10647.
(54) Wertz, C. F.; Santore, M. M. Fibrinogen adsorption on hydrophilic and hydrophobic surfaces: Geometrical and energetic aspects of interfacial relaxations. *Langmuir* **2002**, *18*, 706−715.
(55) Clark, A. J.; Kotlicki, A.; Haynes, C. A.; Whitehead, L. A. A new model of protein adsorption kinetics derived from simultaneous measurement of mass loading and changes in surface energy. *Langmuir* **2007**, *23*, 5591−5600.
(56) Li, L.; Chen, S.; Zheng, J.; Ratner, B. D.; Jiang, S. Protein adsorption on oligo(ethylene glycol)-terminated alkanethiolate self-assembled monolayers: The molecular basis for nonfouling behavior. *J. Phys. Chem. B* **2005**, *109*, 2934−2941.
(57) Kenausis, G. L.; Vörös, J.; Elbert, D. L.; Huang, N.; Hofer, R.; Ruiz-Taylor, L.; Textor, M.; Hubbell, J. A.; Spencer, N. D. Poly(l-lysine)-g-poly(ethylene glycol) layers on metal oxide surfaces: Attachment mechanism and effects of polymer architecture on resistance to protein adsorption. *J. Phys. Chem. B* **2000**, *104*, 3298−3309.
(58) Dalsin, J. L.; Lin, L.; Tosatti, S.; Vörös, J.; Textor, M.; Messersmith, P. B. Protein resistance of titanium oxide surfaces modified by biologically inspired mPEG−DOPA. *Langmuir* **2004**, *21*, 640−646.
(59) Gillich, T.; Benetti, E. M.; Rakhmatullina, E.; Konradi, R.; Li, W.; Zhang, A.; Schlüter, A. D.; Textor, M. Self-assembly of focal point oligo-catechol ethylene glycol dendrons on titanium oxide surfaces: Adsorption kinetics, surface characterization, and nonfouling properties. *J. Am. Chem. Soc.* **2011**, *133*, 10940−10950.
(60) Beurer, E.; Venkataraman, N. V.; Sommer, M.; Spencer, N. D. Protein and nanoparticle adsorption on orthogonal, charge-density-versus-net-charge surface-chemical gradients. *Langmuir* **2012**, *28*, 3159−3166.
(61) Wang, I. W.; Anderson, J. M.; Jacobs, M. R.; Marchant, R. E. Adhesion of Staphylococcus epidermidis to biomedical polymers: Contributions of surface thermodynamics and hemodynamic shear conditions. *J. Biomed. Mater. Res.* **1995**, *29*, 485−493.
(62) Fang; Szleifer, I. Effect of molecular structure on the adsorption of protein on surfaces with grafted polymers. *Langmuir* **2002**, *18*, 5497−5510.
(63) Satulovsky, J.; Carignano, M. A.; Szleifer, I. Kinetic and thermodynamic control of protein adsorption. *Proc. Natl. Acad. Sci. U.S.A.* **2000**, *97*, 9037−9041.
(64) Waite, H. J.; Tanzer, M. L. Polyphenolic substance of Mytilus edulis: Novel adhesive containing L-Dopa and hydroxyproline. *Science* **1981**, *212*, 1038−1040.
(65) Lee, H.; Dellatore, S. M.; Miller, W. M.; Messersmith, P. B. Mussel-inspired surface chemistry for multifunctional coatings. *Science* **2007**, *318*, 426−430.
(66) Ham, H. O.; Liu, Z.; Lau, K. H. A.; Lee, H.; Messersmith, P. B. Facile DNA immobilization on surfaces through a catecholamine polymer. *Angew. Chem., Int. Ed.* **2011**, *50*, 732−736.
(67) The effective diameter (D) of the DOPA-Lys pentapeptide segment was estimated from the aggregate geometric volumes of the five amino acids = 0.9 $nm^3 = \pi D^3/6$.
(68) Gorbet, M. B.; Sefton, M. V. M. V. Biomaterial-associated thrombosis: roles of coagulation factors, complement, platelets and leukocytes. *Biomaterials* **2004**, *25*, 5681−5703.
(69) Saxer, S.; Portmann, C.; Tosatti, S.; Gademann, K.; Zuercher, S.; Textor, M. Surface assembly of catechol-functionalized poly(L-lysine)-graft-poly(ethylene glycol) copolymer on titanium exploiting combined electrostatically driven self-organization and blomimetic strong adhesion. *Macromolecules* **2010**, *43*, 1050−1060.
(70) Pei, J.; Hall, H.; Spencer, N. D. The role of plasma proteins in cell adhesion to PEG surface-density-gradient-modified titanium oxide. *Biomaterials* **2011**, *32*, 8968−8978.
(71) Sherertz, R. J.; Sarubbi, F. A. A three-year study of nosocomial infections associated with Pseudomonas aeruginosa. *J. Clin. Microbiol.* **1983**, *18*, 160−164.
(72) Pierce, G. E. Pseudomonas aeruginosa, Candida albicans, and device-related nosocomial infections: implications, trends, and potential approaches for control. *J. Ind. Microbiol. Biotechnol.* **2005**, *32*, 309−318.
(73) Kingshott, P.; Wei, J.; Bagge-Ravn, D.; Gadegaard, N.; Gram, L. Covalent attachment of poly(ethylene glycol) to surfaces, critical for reducing bacterial adhesion. *Langmuir* **2003**, *19*, 6912−6921.